

# Epidemics and Percolation

Lavinia Thimm, Luka Vomberg\*

## I. INTRODUCTION

The simulation of epidemic outbreaks plays a crucial part in understanding the ways diseases spread through a population and finding appropriate countermeasures. It can be used to evaluate which type and degree of countermeasures lead to a slowing of the spread of the disease. One prominent example is the reduction of physical contact between individuals, the so called 'social distancing'. This can prolong the development of the epidemic, which alleviates pressure from the health care systems. In the recent news concerning the Covid-19 outbreak, this is widely referred to as 'flattening of the curve' [1]. Due to their current relevance, this project is focused on the impact of such interventions.

The first step in simulating the spread of an epidemic via contact between infective and susceptible individuals in a population is finding a model for said population. Focusing on two important properties of real populations, namely 'clustering' and 'small-world' effects, the simulation presented takes the same general approach as [2]. Individuals and their contacts are represented by sites on a 2-dimensional lattice with nearest-neighbor bonds with periodic boundary conditions and some additional shortcuts. Furthermore the lattice sites are assigned an age depending on the current age distribution of Germany [3], which determines the susceptibility to the disease.

As epidemic model the widespread susceptible/infective/removed 'SIR' model is chosen. It defines the disease and its propagation via susceptibility and transmissibility, the probability that an exposed individual will contract the disease and the probability that the contact between two individuals will lead to exposure to the disease. Simulating the outbreak of an epidemic can be closely related to the percolation problem, defining the susceptible lattice sites as occupied sites and bonds that lead to transmission of the disease as occupied bonds. If these are randomly distributed the problem of whether an epidemic takes place on a large scale can be interpreted as a percolation problem where a percolating cluster forms if at least a critical fraction  $p_c$  of sites or bonds is occupied. [2]

The simulation starts with one randomly chosen infective individual, the 'patient 0', and then simulates a propagated outbreak.

Current research on epidemics suggest that both social distancing and vaccination show great potential in fighting diseases of many kinds [4, 5].

In addition to evaluating the impact of both measures on the outbreak properties on the 2-dimensional small-world network, this research focuses on how these measures might complement each other or whether at some point one makes the other unnecessary. For this purpose the spread of an epidemic is simulated for a range of initial immunity quotas and social distancing parameters on the same network.

We show the effects that vaccination of a population results in herd immunity effects, and compare social distancing measures to it. It is concluded, that social distancing has a small effect on the total amount of people infected by a disease. However the number of concurrently infected individuals does decrease with higher social distancing. Furthermore we show that there is a phase transition in epidemic outcomes on the parameter space of these two countermeasures. We conclude that social distancing is a viable countermeasure to a disease for which no vaccine is available.

The outline of the paper is as follows. First the percolation problem as such is examined, then its relation to the study of the SIR epidemic model is discussed and the studied model is described in detail in section II. The algorithms and simulation approach are described in section III. In section IV the simulation results are compiled and discussed in section V. A short summary including an outlook with further possible improvements to the simulation is given in section VI.

## II. THEORETICAL BASIS

### A. Percolation

Percolation (from latin *percolare*: *trickle through*) originally describes the trickling of a fluid through a porous medium. The words fluid and medium are to be taken in their widest sense. For example filtering coffee is a percolation process, the water being the liquid and the ground up coffee being the medium, but it could also be that the liquid is an infectious disease and the medium the population it spreads on.[6]

To understand the principles it is useful to look at the problem as a purely geometrical one. Let there be a general network that consists of sites and bonds between them. Each site can now be either occupied or not with probabilities  $p$  or  $1-p$  respectively. Occupied sites which are connected are said to form a cluster in the *site* percolation problem. Alternatively in *bond* percolation the bonds between the sites are either occupied or vacant.[6]

One quantity that is of interest in this problem is the percolation threshold  $p_c$ . In an infinitely large network

---

\* [s6lathim@uni-bonn.de](mailto:s6lathim@uni-bonn.de), [s6luvomb@uni-bonn.de](mailto:s6luvomb@uni-bonn.de)

there exist only finite clusters for  $p < p_c$ , while for  $p \geq p_c$  there exist a cluster spanning from one boundary of the lattice to the other [7]. The exact value of  $p_c$  is of course dependent on the geometry of the network in question. In the most simple case of a 1 dimensional chain of sites it is obvious that  $p_c = 1$  for bond and site percolation. But even in a 2 dimensional regular lattice the site percolation threshold has to be calculated through simulation.

The connection of this geometric model to epidemics is as follows: the sites can be interpreted as individuals, whose contacts with each other are the bonds. Each individual has some contacts with others. These contacts can be either infectious, in which case the bond can be said to be occupied, or non infectious, which means the bond stays vacant. The individuals can thus connect to a cluster. If any one of the individuals carry an infection every other individual in the same cluster will contract it as well. If the density of infectious contact is above  $p_c$  a disease can potentially spread through the entire population.

The basic ideas of percolation theory can be refined and used for epidemic models that more closely resemble reality. Firstly it is possible to combine bond and site percolation by considering that some individuals might be immune. A real disease does not spread instantly, but over time. This means that the occupation of bonds also has to be time dependent. Furthermore an infected person will not stay infected indefinitely, but will recover or die at some point. Such considerations lead quite naturally to the development of SIR type models.

## B. SIR

The SIR (Susceptible, Infected, Removed) model is based on the observation that epidemic infections spread by one infective individual infecting others with a rate  $x$  per contact and recovering or dying after time  $\tau$ . Applying this simple approach on a fully conjugated graph leads to differential equations in 1 to describe the spread of the disease.

$$\frac{\partial S}{\partial t} = -x \frac{I}{N} S \quad \frac{\partial I}{\partial t} = x \frac{I}{N} S - \frac{I}{\tau} \quad (1)$$

Where from  $N$  sites on a lattice, the number of infected sites  $I(t)$  infect the remaining number of susceptible sites  $S(t)$  each at a rate  $x/N$  and are removed at a rate  $1/\tau$ . An outbreak of a disease is observed if  $\frac{\partial I}{\partial t} > 0$  at  $t = 0$ . This evaluates to the definition of the basic reproductive number  $R_0 = xS(0)\tau/N$  characterizing the disease: if  $R_0 > 1$  an outbreak may or may not occur, for  $R_0 \leq 1$  the disease does not break out. [8]

Transferring this model to a 2-dimensional small-world network with shortcuts makes it impossible to write such easy differential equations, however the interpretation still holds, see [9, 10, 11].

In the simulation the infection rate  $x$  is replaced by a transmissibility  $p_{\text{trans}}$  defining the probability that the contact between two individuals will lead to exposure to

the disease and the susceptibility  $p_{\text{susc}}$  that an exposed individual will contract the disease. Starting with one infected individual 'patient 0' the progress of the epidemic is simulated in time steps until there are no more infected individuals. This approach is based on the recovered being permanently removed from the pool of susceptible individuals. Slight variations of the SIR model also include returning to being susceptible after a given period of time.

Two sets of susceptibility distributions are used. In the first the distribution is set rather arbitrarily to  $p_{\text{susc}} = 0.7$ , such that individuals are highly susceptible to the disease. For defining the second distribution, each individual is assigned an age, see table I, approximated according to the age distribution of Germany 2018 [3]. Taking into account that the immune system peaks at the ages of 20–40 the susceptibility is set for each age group accordingly, to see if such a difference has a large impact on the overall result. To be comparable to  $p_{\text{susc}} = 0.7$  the range of susceptibilities is chosen with a weighted mean of 0.7, see table I.

age	0–3	3–20	20–40	40–60	60–80	80+
quota	3%	15%	25%	28%	22%	7%
susceptibility	0.98	0.70	0.45	0.70	0.85	1.00

Table I: Age Distribution quota of the population for the different age groups [3] and the correspondingly chosen susceptibilities.

Starting with a 100% transmissible disease,  $p_{\text{trans}} = 1$ , the simulation then includes a factor  $1/D$  to implement the impact of social distancing on the spread of the disease. Meaning e.g. reducing the social contacts of all individuals to half of what they were before ( $D = 2$ ) leads to  $p_{\text{trans}}[\text{new}] = p_{\text{trans}}[\text{old}]/D = 0.5$ . The spreading of diseases for  $D \in \{1–7\}$  in steps of 0.2 is simulated.

Transmissibility and susceptibility are chosen independent of each other such that instead of testing two probabilities only the product  $p = p_{\text{trans}} \cdot p_{\text{susc}}$  will be tested against a uniform random number in the simulation.

Any infected individual can be removed, effectively by changing the susceptibility to 0, either by recovery or death, the probability for both is represented by one recovery distribution. In resemblance to influenza-like diseases the probability is not fixed for each time step, rather a random value from a normal distribution with mean  $\mu = 6$  and standard deviation  $\sigma = 2$  is compared to the time the individual is already infected.

Testing the impact of immunity in the initial population, either naturally occurring or through vaccination, is realized by randomly setting a portion of the susceptible individuals corresponding to the desired vaccination ratio  $r$  as removed via changing their susceptibility to 0. Thus the initially removed individuals are given by  $R = r \cdot N$ . The simulation is performed for  $r \in \{0–0.5\}$  in steps of 0.02.

### C. Relevant Observables

The development and impact of an epidemic can be characterized by the number of infected individuals.

The total quota of infected individuals during an epidemic is called the 'size' of the epidemic.

From this the outbreak of a major epidemic (ME) is defined if the size is larger than a fixed percentage of the susceptible population. There is no predefined distinction between major and minor epidemics on finite networks [4, 2], however the impact of infecting 2% of a population in total can be considered major. Thus, for multiple simulation runs the probability for a major epidemic can be determined by setting ME = 1 for size > 2% and to 0 otherwise. The mean over all ME then yields the probability for a major epidemic P(ME).

The number of concurrently infected individuals at time  $t$ ,  $I(t)$ , is inherent to the SIR model and forms a basis for calculating the following observables. The impact of an epidemic is largely determined by the number of concurrently infected individuals  $I_{\max}$ , as it determines the maximal strain put on the health care system by the epidemic.

As defined in II B the basic reproductive number  $R_0$  defines whether an epidemic can break out ( $R_0 > 1$ ) or won't break out ( $R_0 \leq 1$ ). In the 2 dimensional lattice model with all above mentioned modifications and dependencies the simple definition from differential equations can no longer be applied. It is instead determined from the fractional increase of infected individuals from one time step to the next, see [12]. For clarification we denote this as  $R_0 * (t) = I(t+1)/I(t)$ , which can be calculated for any given time step<sup>1</sup>.

Where it is not further specified the observables are obtained by taking the mean of the measured or calculated observables from 100 simulations with the same disease parameters. The errors are then obtained via bootstrapping from the observables.

## III. METHODS

The whole simulation and evaluation code can be found on gitHub<sup>2</sup>. We started building our R simulation code by first writing an algorithm that is able to efficiently examine clusters in a given lattice. For this we chose a "weighted union find algorithm with path compression" as it is presented by Newman and Ziff in [13]. This type of algorithm checks if 2 sites are connected. There are 3 possible outcomes of this check. Firstly if the sites were previously not in any cluster it assigns one as the root of a

new tree to which the other is added as a node. Secondly if one of the sites is already part of a cluster and the other is not, the single site as amalgamated to the root node of the first. Thirdly when both sites are already part of a tree the root of the smaller tree is amalgamated to the root of the larger (weighted). Whenever single sites or trees need to be joined it is necessary to traverse the tree they are joined to. Whenever this is done all traversed elements are then added to the root node directly, which shortens the time needed to traverse the tree the next time. Usually a lattice with a certain  $p$  is created and then the observables  $Q_p$  of interest are measured, which needs to be repeated for many values of  $p$  and each time the above algorithm will need to be used from the start. The method Newman and Ziff proposed is that instead the lattice can be populated by one bond at a time. Each time a bond is added the above algorithm decides what needs to be done and does it. This means it only ever has to do one step per bond.

This algorithm was implemented and tested. To verify it is working correctly we used it to estimate  $p_c$  for bond percolation on a 2D square lattice which is known analytically to be 0.5 which we were able to confirm. We were also able to verify the computation time to be of  $O(N)$ .

To make the algorithm applicable to the SIR model simulation we changed the algorithm to not add bonds randomly, but between the individuals which transmit a disease. Furthermore the infected individuals are assigned a variable each which keeps track of how long they have been infected already. At the end of each time step it is checked which individuals successfully pass the recovery test.

In [2] the approach is to represent the population of  $N$  people by a 1-dimensional chain, where the infection can pass through the bonds of the chain, creating the 'clustering' behavior also observed in real populations. This leads to an increased probability of two people having mediated contact if they have a common acquaintance opposed to a random graph, where it is uniform for all cases.

In real populations another well-observed behavior is the 'small-world' effect, meaning that any two people can be connected via a small number of acquaintances ( $\approx 6$ ). This property leads to a much faster disease propagation compared to regular lattices.

These properties are achieved by adding a small number of random shortcuts to the chain [2]. This ansatz is used here as well, a but a 2D square lattice is used. This has the advantage of being easier to visualize, which was very helpful in debugging the code. For reproducibility of the results and for keeping the same lattice and shortcut configurations for any simulation the simulation seed is set to 1. For all results presented the lattice has  $N = 160000$  sites,  $N/100$  shortcuts and periodic boundary conditions. With these parameters the mean distance between 2 people is 33(6).

It is also possible to supply the code with any other

<sup>1</sup> Another commonly used definition of  $R_0$  is the total number of people one typical infective individual infects over the whole time it is carrying the disease. This definition holds the same transition at 1 but yields different numeric values.

<sup>2</sup> <https://github.com/lthUniBonn/epidemics.git>

arbitrary network, as long as the connections are defined via the nodes they connect the simulation including the evaluation can be performed.

This representation of a population leads to systematic uncertainties in the generated results based on the strong variation in the number of connections in a real population as opposed to a lattice with a small amount of shortcuts [12]. The impact of this discrepancy cannot be quantified reasonably, as it can lead to a bias in both enhanced and hindered disease propagation. It can especially enlarge the difference in outcomes for one disease depending on the starting environment.

Another downside of our approach is, that a single person can only infect a very limited number of others depending on the dimensionality of the lattice and the number of shortcuts. Therefore infectiousness is capped by the number of connections of each individual.

Since for one set of parameters the simulation is run 100 times, it is necessary to take the mean results for each observable. The resulting values for the observables are not normally distributed in general. This is to be expected, as there are runs where a disease dies out very quickly due to a statistical fluke, but when the same disease survives long enough to infect some people it is basically impossible for it to die out quickly just by chance. This then results in bimodal distributions of some of the observables. Due to this the standard error of the mean is computed via bootstrapping as discussed in [14]. In short bootstrapping consists of repeated resampling of a given sample of an unknown population with replacement and considering the sample as an estimator of the population. The error of the observable obtained from the sample is then given by the standard deviation of the observables obtained from the resamples. This determination of the error is only valid if the distribution of resampled observables closely matches the normal distribution, which is found to be the case via qq-plots.

Furthermore the bias, meaning the difference between the original observable and the mean of the resampled observables, has to be much smaller than the obtained error, which is also found to be true for our case.

## IV. RESULTS

We use the methods mentioned above to simulate the spread of an epidemic for different values of the immunity, social distancing as well as for 2 types of susceptibility distributions. For each set of parameters the simulation is done 100 times to reduce the statistical error. If not stated otherwise the data in the graph is given as the mean result of these 100 runs and the errors are the standard errors of the mean derived by bootstrapping. For data points which do not have errors given, this is because there was only 1 run left, e.g. at a late time step when only 1 out of 100 illnesses is still spreading a statistical error can not be calculated. All the data shown in IV A-IV D used the first of the susceptibility distributions

given in section II B.

### A. Visual presentation of outbreaks

First we want to give the reader the possibility to watch some epidemics spread on our lattice. The first frame displays a disease ( $r = 0.14$ ,  $D = 4$ ) that spreads very quickly to almost the entire population, see figure 1. The second frame shows a disease ( $r = 0.2$ ,  $D = 4$ ) that spreads more slowly and affects less of the population, see figure 2. The last frame shows a disease that dies out after the first few steps ( $r = 0.2$ ,  $D = 4.7$ ), see figure 3. The individuals marked by the red stars are the ones currently infected while the black dots are recovered.

Figure 1: Spread of epidemic ( $r = 0.14$ ,  $D = 4$ )  
red: currently infectious, black: recovered,  
white: not affected (start on click)

### B. Concurrently Infected

The first observable of interest is the number of concurrently infected people  $I(t)$ . The respective time series is displayed in figure 4. The two curves were created with the same set of parameters except for the social distancing  $D$ . In figure 5 the same is done for different immunization quotas  $r$ .

To further analyze how  $I(t)$  changes depending on  $r$  and  $D$ , the maximal number of concurrently infected  $I_{\max}$  for a range of  $r$  or  $D$  is shown in figures 6 and 7 for two different values of the fixed parameter  $D$  or  $r$ , respectively.

Figure 2: Spread of epidemic ( $r = 0.2$ ,  $D = 4$ )  
 red: currently infectious, black: recovered,  
 white: not affected (start on click)

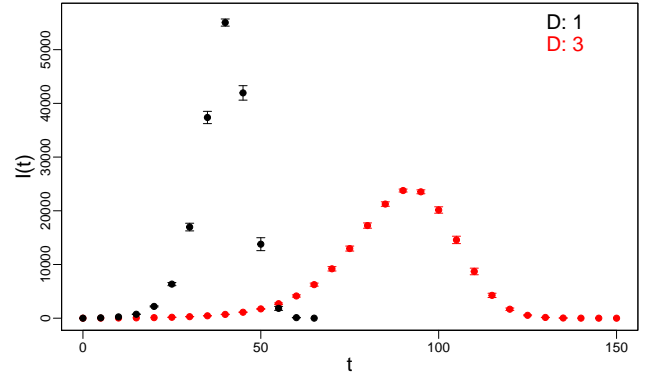


Figure 4: The number of currently infected individuals  $I(t)$  is shown for different social distancing values,  $r = 0$

Figure 3: Spread of epidemic ( $r = 0.2$ ,  $D = 4.7$ )  
 red: currently infectious, black: recovered,  
 white: not affected (start on click)

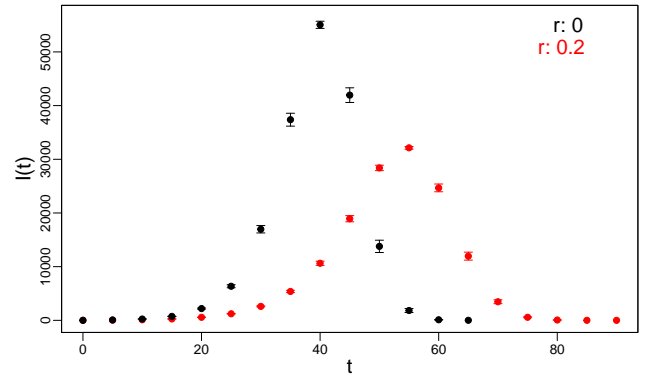


Figure 5: The number of currently infected individuals  $I(t)$  is shown for different immunity values,  $D = 1$

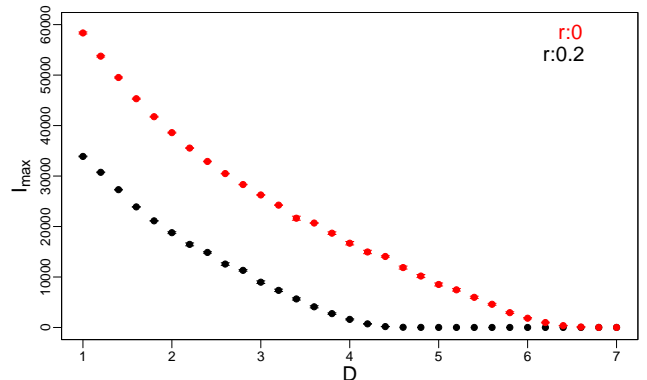


Figure 6: The number of the maximal concurrently infected individuals  $I_{\max}$  is shown as a function of social distancing  $D$ .

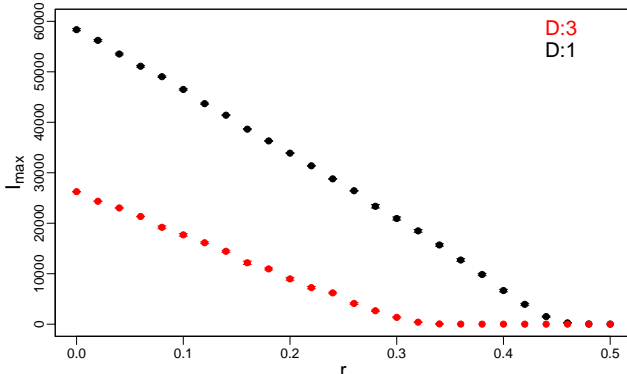


Figure 7: The number of the maximal concurrently infected individuals  $I_{\max}$  is shown as a function of immunity  $r$ .

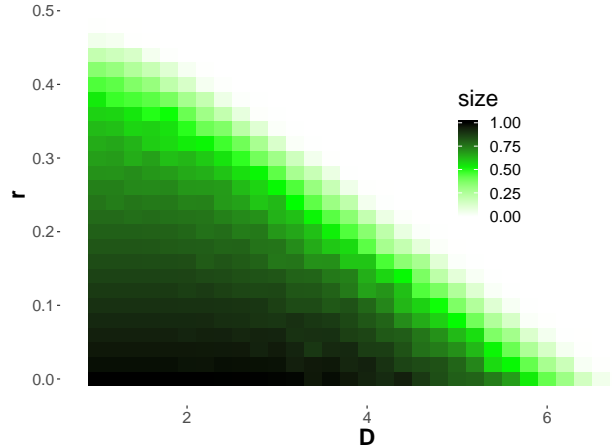


Figure 9: The size of the epidemic depending on  $r$  and  $D$  is shown.

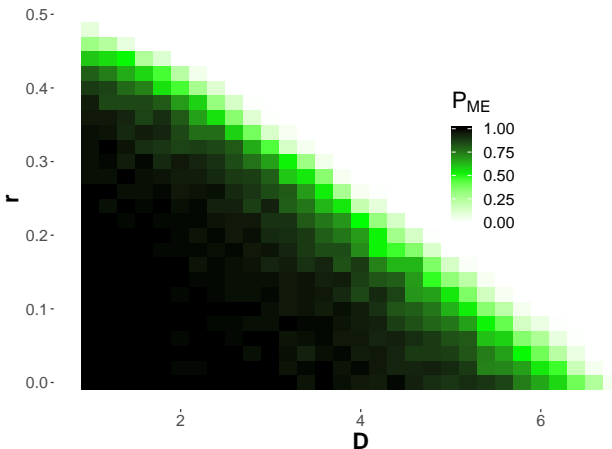


Figure 8: The probability of a major outbreak  $P_{ME}$  depending on  $r$  and  $D$  is shown.

### C. Epidemic Outcomes

The impact on the outcome of the epidemic by a combination of vaccination and social distancing is shown in figures 8 and 9 giving the probability for a major epidemic or the size of the epidemic as a measure of impact.

Slices of the heat map for the epidemic size, see figures 11 and 10, and for  $P_{ME}$ , see figures 12 and 13, are displayed, showing their development depending on the parameters in more detail including error information. The range of errors is similar for all other slices. In some cases the errors are extremely small such that they cannot be displayed properly.

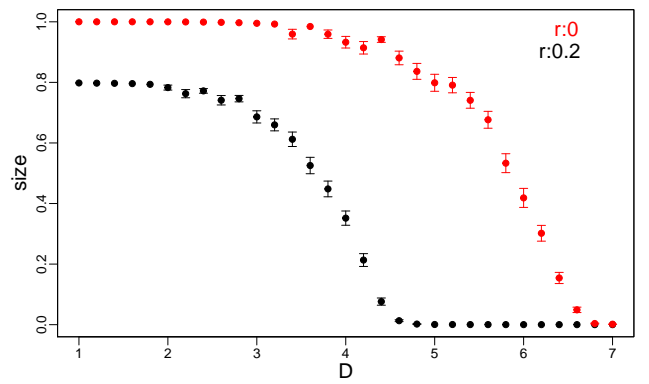


Figure 10: The size of the epidemic depending on the social distancing  $D$  is displayed for two parameter configurations.

### D. $R0^*$

$R0^*$  was determined for all time steps for a typically major, moderate and fast-dying epidemics, see figures 14,15 and 16, respectively. As  $R0^*$  can only be computed from ongoing runs at time  $t$ , the proportion of the simulation runs that were used in the computation is displayed in the same graph as red data points.

### E. Age Dependent Susceptibility Distribution

The same procedure that was used to obtain the results above is repeated for the second age distribution, with the difference of only running the simulation 20 times per parameter set. This is done to be able to gauge the magnitude of the difference the more diverse distri-

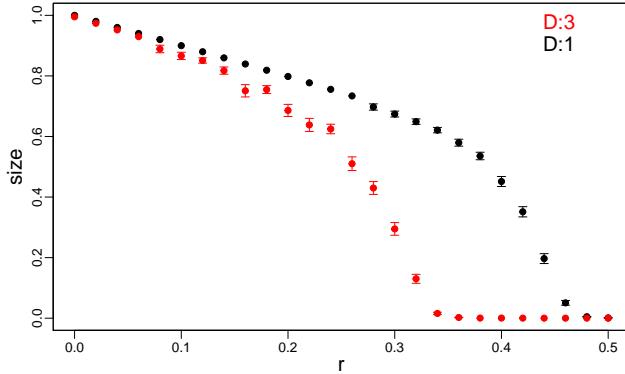


Figure 11: The size of the epidemic depending on the vaccination quota  $r$  is displayed for two parameter configurations.

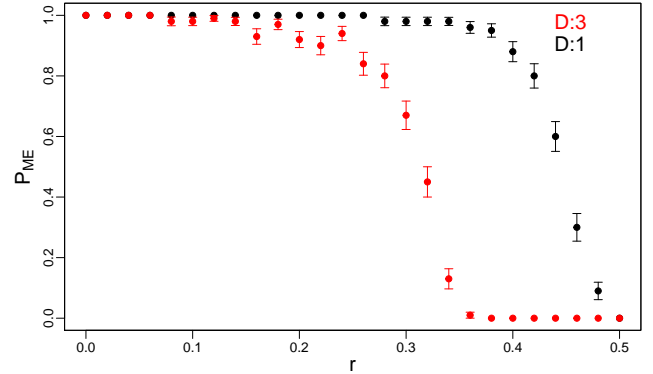


Figure 13: The probability of the epidemic outbreak depending on the vaccination quota  $r$  is displayed for two parameter configurations.

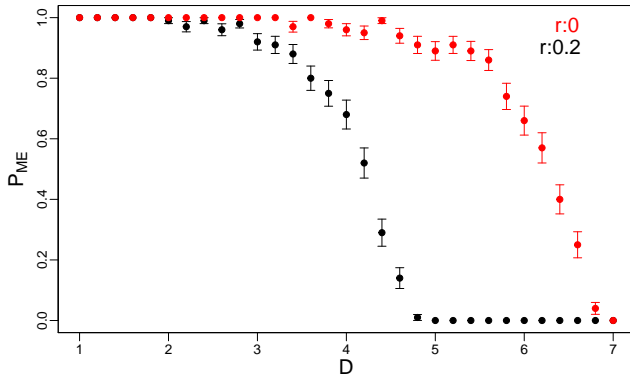


Figure 12: The probability of the epidemic outbreak depending on the social distancing  $D$  is displayed for two parameter configurations.

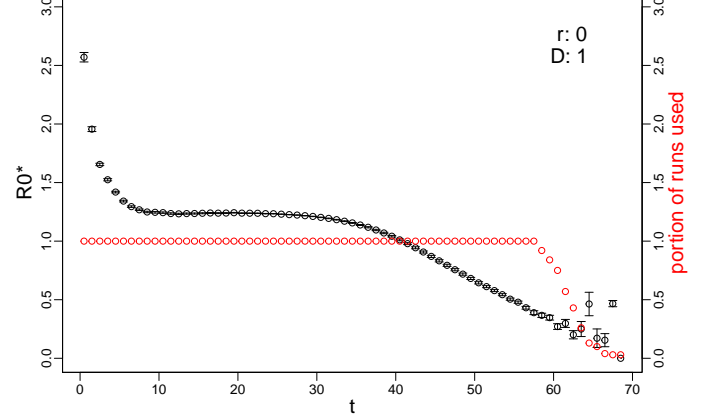


Figure 14:  $R0^*$  for all time steps for  $r = 0.0$  and  $D = 1$ . Red points give the respective proportion of simulation runs used in the calculation.

bution makes, before investing more computation time than necessary. As an example of the second set of data the analogous heat maps to figures 8 and 9 are given in figure 17.

## V. DISCUSSION

The overall impact of both vaccination and social distancing measures can be well observed in the visual differences in propagation of the diseases in figures 1, 2 and 3.

The impact of social distancing on the number of concurrently infected over time shows already a clear reduction in the maximal number of concurrently infected as well as the typically expected 'flattening' and 'broaden-

ing' of the curve, see figure 4. Similar to this, vaccination also reduces the number of maximally infected, however a similarly significant 'broadening' is not observed, see figure 5. The reduction of the maximally infected is crucial in evaluating countermeasures to a disease, as the health care system can only take a limited number of infected before not being able to treat all patients in need of care. Such a situation is to be avoided as much as possible, meaning that potential countermeasures are expected to reduce  $I_{\max}$  significantly. The reduction to be expected from either social distancing or vaccination is shown in figure 6 and 7. Both measures show a significant impact on  $I_{\max}$ , while for social distancing the regime from  $D \in 1-2$  shows a very strong reduction followed by more and more flattened reduction for higher  $D$ , vaccination shows strong linear reduction.

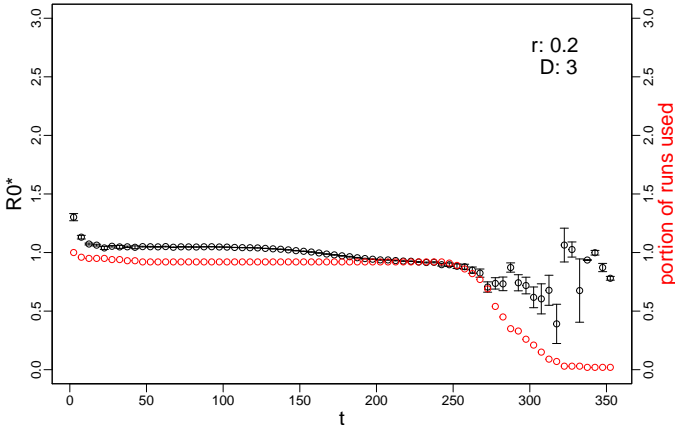


Figure 15:  $R0^*$  for all time steps for  $r = 0.2$  and  $D = 3$ . Red points give the respective proportion of simulation runs used in the calculation.

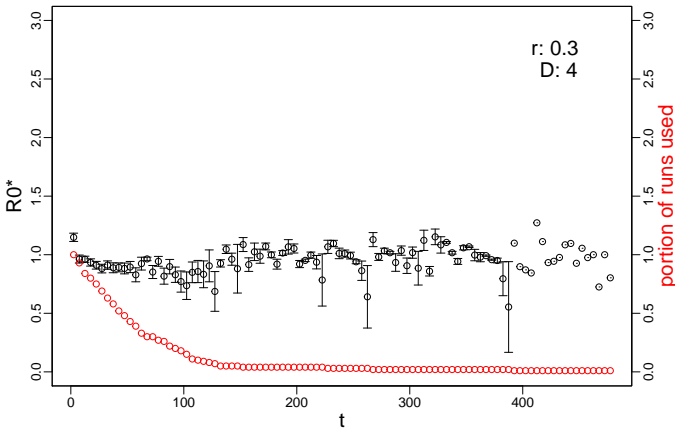


Figure 16:  $R0^*$  for all time steps for  $r = 0.3$  and  $D = 4$ . Red points give the respective proportion of simulation runs used in the calculation.

Both measures combined, see figures 8 and 9, show a clear phase transition line separating the parameter region where the probability for a major epidemic is close to 1 and the region without major epidemics, which also shows the connection from epidemics to the percolation probability phase transition. Social distancing of  $D \approx 6$  leads to the disease dying out instantly, as the transmission of the disease becomes very unlikely. The value of this threshold is governed by the susceptibility as well as the recovery time available for infectious contact.

The commonly known concept of herd immunity [15] can be observed distinctly and visibly, as by vaccination of 50% of the population the probability for a major epidemic is approximately 0. A beginning of this effect can be observed in the more nuanced graph giving the size of the epidemic. For social distancing the size always

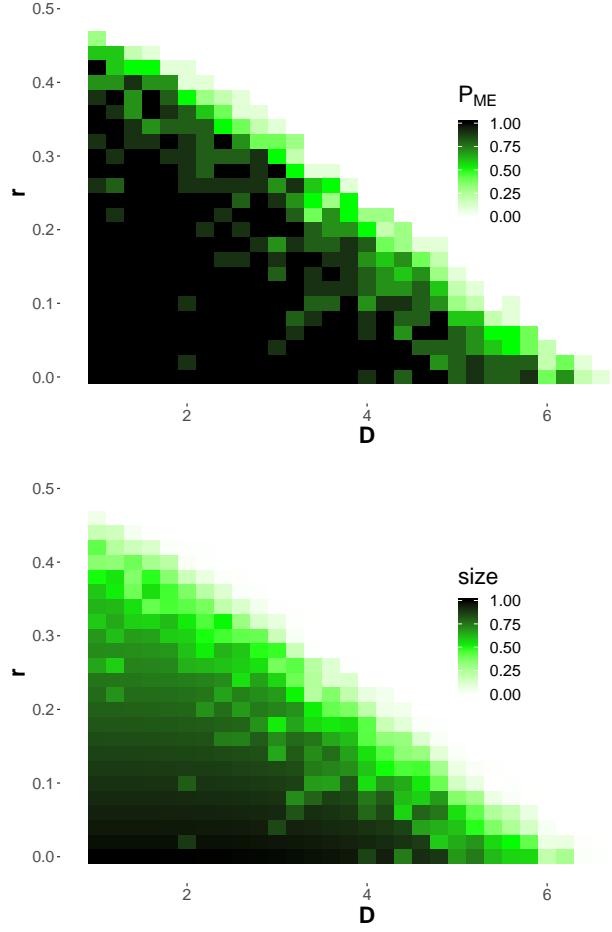


Figure 17: The probability of a major outbreak  $P_{ME}$  (top) as well as the size of the epidemic (bottom) depending on  $r$  and  $D$  is shown for the second susceptibility distribution as given in table I.

gets close to 1, meaning that even though the epidemic was prolonged and the maximal number of concurrently infected individuals was reduced, with enough time still  $\approx 100\%$  of susceptible individuals were infected. Due to herd immunity effects, the size of the epidemic decreases gradually for rising immunity quotas, meaning that already some individuals are protected from the disease despite being susceptible. This behavior can also be observed in more detail in figures 12 and 13 for the similar trend in  $P_{ME}$  and the direct decrease in size for vaccination compared to the constant size for social distancing in figures 10 and 11.

Vaccination is well known to be highly effective in the fight against diseases [15, 4], we were able to reproduce this behavior in the model used and also clearly show herd immunity effects. We have shown that social distancing, whilst being a lot more inconvenient, has a very similar effect on the maximal number of concurrently infected, which can be used to slow and spread the outbreak of diseases when no vaccine is available. In addition even

small amounts of social distancing are found to have a significant stalling effect already. Strict measures of social distancing, especially with the effect of prolonging the disease while lessening the effects, thus pose a much stronger strain on the population than vaccination, they are however valuable if no alternative vaccine is available.

The determination of  $R0^*$  and the possible interpretations were investigated. However in the scenario of only one initially infective individual, determining  $R0^*$  of diseases which die out quickly is lined with some problems.  $R0^*$  was determined for all time steps for each run, then the mean  $R0^*$  for each time step of all runs was investigated to see if it shows a distinct development. For a strongly spreading disease, see figure 14, the change from  $R0^* > 1$  for an expanding disease to dying out some time after  $R0^* < 1$  is observed. In this case most diseases survive until  $t \approx 60$  and then abruptly die out, such that from this point onward  $R0^*$  can only be determined from the surviving diseases. This leads to a problem in determining an unbiased  $R0^*$  for moderate and fast-dying diseases as only the small number of surviving diseases can contribute, which always realize  $R0^* \geq 1$ , see figures 15 and 16, respectively. Determining  $R0^* < 1$  for fast-dying diseases is therefore not possible in this model. However in a model that starts with more than one patient 0, this distinction is predicted to work, also from the behavior of the strongly spreading disease, where such an  $R0^* < 1$  is measurable without any problems.

Determining the behavior of the epidemic and interventions depending on  $R0^*$ , especially in comparison to the probability of a major epidemic  $P_{ME}$  is therefore, for this specific case of one patient 0, not further discussed.

The plots shown in figure 17 and 8/9 are very similar qualitatively. The major difference is, that the second plot is not as smooth. At this point it is not clear how much of this is due to the lower number of samples (20 vs 100) and how much due to the more diverse susceptibility distribution. However since the plots are very similar in the general behavior concerning the interventions, we decided not to further investigate this matter.

When thinking about the errors in the model and how it relates to reality the statistical errors, while significant, are not as important to keep in mind as the systematic uncertainties made when simplifying a complex social network to a square lattice as well as the complex properties of susceptibility and transmissibility of a disease to fixed probabilities for each individual.

## VI. SUMMARY

The spread of an epidemic on a 2d nearest neighbor lattice which has the small world property is simulated using the SIR model, gauging the impact of both immunity and social distancing.

The effects of both countermeasures are observed to be reduction of the maximal concurrently infected in both cases and for immunity due to herd immunity effects also

a reduction of the epidemic size. We conclude that social distancing is a viable alternative to vaccination as epidemic countermeasure, when no vaccines are available.

The results are mainly limited by the model chosen for the population, a static network is not an exact image of a society, however it was modeled after a real population taking into account its properties of 'clustering' and 'small-world' effects. Additionally the disease parameters are arbitrarily set. This supports that a qualitative result for an overall effect can be drawn, results with a quantitative character would necessitate a closer orientation to a real disease.

## Outlook

Further improvements to the discussed simulation model could be added, such as a higher dimensional lattice, next nearest neighbor interactions as well as more complex networks. Provided all possible bonds are given, this would only need very minor adjustments in the simulation.

An important handle on the impact of the discussed countermeasures would be to implement them with a specified time delay. This delay could depend on the proportion of individuals infected to test how the countermeasures impact an already ongoing epidemic.

Another possibility is to allow for the loss of immunity that is gained after contracting the disease once. This would mean that individuals can be affected multiple times, which could lead to waves of infection, as seen in some real world influenza diseases.

The simulation also yields information on the clustering of infected individuals, which might lead to a structural analysis of the impact of the countermeasures.

## REFERENCES

- [1] European Centre for Disease Prevention and Control. *Guide to public health measures to reduce the impact of influenza pandemics in Europe – ‘The ECDC Menu’*. URL: <https://www.ecdc.europa.eu/en/publications-data/guide-public-health-measures-reduce-impact-influenza-pandemics-europe-ecdc-menu> (visited on 03/26/2020) (cit. on p. 1).
- [2] Christopher Moore and M. E. J. Newman. “Epidemics and percolation in small-world networks”. In: *Phys. Rev. E* 61 (5 May 2000), pp. 5678–5682. DOI: [10.1103/PhysRevE.61.5678](https://doi.org/10.1103/PhysRevE.61.5678). URL: <https://link.aps.org/doi/10.1103/PhysRevE.61.5678> (cit. on pp. 1, 3).
- [3] Statistisches Bundesamt. *Population in Germany*. 2019. URL: <https://service.destatis.de/bevoelkerungspyramide/#!y=2018&a=3,20&v=2&l=en&g> (visited on 03/10/2020) (cit. on pp. 1, 2).

- [4] Eben Kenah and Joel C Miller. “Epidemic Percolation Networks, Epidemic Outcomes, and Interventions”. In: *Interdisciplinary Perspectives on Infectious Diseases* 2011 (2011). ISSN: 1687-708X. URL: <http://www.hindawi.com/journals/repid/2011/543520/abs/> (cit. on pp. 1, 3, 8).
- [5] Fong MW et al. “Nonpharmaceutical Measures for Pandemic Influenza in Nonhealthcare Settings—Social Distancing Measures”. In: *Emerg Infect Dis.* 26 (5 May 2020), to appear. DOI: [10.3201/eid2605.190995](https://doi.org/10.3201/eid2605.190995). URL: <https://doi.org/10.3201/eid2605.190995> (cit. on p. 1).
- [6] Muhammad Sahimi. *Applications of Percolation Theory*. 2009 (cit. on p. 1).
- [7] Dieter W. Heermann Kurt Binder. *Monte Carlo Simulation in Statistical Physics*. 2019 (cit. on p. 2).
- [8] L.M Sander, C.P Warren, and I.M Sokolov. “Epidemics, disorder, and percolation”. In: *Physica A: Statistical Mechanics and its Applications* 325.1 (2003). Stochastic Systems: From Randomness to Complexity, pp. 1–8. ISSN: 0378-4371. DOI: [https://doi.org/10.1016/S0378-4371\(03\)00176-6](https://doi.org/10.1016/S0378-4371(03)00176-6). URL: <http://www.sciencedirect.com/science/article/pii/S0378437103001766> (cit. on p. 2).
- [9] M. E. J. Newman and D. J. Watts. “Scaling and percolation in the small-world network model”. In: *Physical Review E* 60.6 (Dec. 1999), pp. 7332–7342. ISSN: 1095-3787. DOI: [10.1103/physreve.60.7332](https://doi.org/10.1103/physreve.60.7332). URL: <http://dx.doi.org/10.1103/PhysRevE.60.7332> (cit. on p. 2).
- [10] M. E. J. Newman, C. Moore, and D. J. Watts. “Mean-Field Solution of the Small-World Network Model”. In: *Physical Review Letters* 84.14 (Apr. 2000), pp. 3201–3204. ISSN: 1079-7114. DOI: [10.1103/physrevlett.84.3201](https://doi.org/10.1103/physrevlett.84.3201). URL: <http://dx.doi.org/10.1103/PhysRevLett.84.3201> (cit. on p. 2).
- [11] Cristian F. Moukarzel. “Spreading and shortest paths in systems with sparse long-range connections”. In: *Physical Review E* 60.6 (Dec. 1999), R6263–R6266. ISSN: 1095-3787. DOI: [10.1103/physreve.60.r6263](https://doi.org/10.1103/physreve.60.r6263). URL: <http://dx.doi.org/10.1103/PhysRevE.60.R6263> (cit. on p. 2).
- [12] M. E. J. Newman. “Spread of epidemic disease on networks”. In: *Physical Review E* 66.1 (July 2002). ISSN: 1095-3787. DOI: [10.1103/physreve.66.016128](https://doi.org/10.1103/physreve.66.016128). URL: <http://dx.doi.org/10.1103/PhysRevE.66.016128> (cit. on pp. 3, 4).
- [13] M. E. J. Newman and R. M. Ziff. “Efficient Monte Carlo Algorithm and High-Precision Results for Percolation”. In: *Physical Review Letters* 85.19 (Nov. 2000), pp. 4104–4107. ISSN: 1079-7114. DOI: [10.1103/physrevlett.85.4104](https://doi.org/10.1103/physrevlett.85.4104). URL: <http://dx.doi.org/10.1103/PhysRevLett.85.4104> (cit. on p. 3).
- [14] M. Petschlies and C. Urbach. *Lecture script in Computational Physics*. 2019 (cit. on p. 4).
- [15] Tae Kim, Jennie Johnstone, and Mark Loeb. “Vaccine herd effect”. In: *Scandinavian journal of infectious diseases* 43 (May 2011), pp. 683–9. DOI: [10.3109/00365548.2011.582247](https://doi.org/10.3109/00365548.2011.582247) (cit. on p. 8).